

# Efficient Domain Adaptation for Endoscopic Visual Odometry

Junyang Wu<sup>1</sup> Yun Gu<sup>1</sup> Guang-Zhong Yang<sup>1</sup>

<sup>1</sup>Institute of Medical Robotics, Shanghai Jiao Tong University, Shanghai, CHINA.

**Abstract.** Visual odometry plays a crucial role in endoscopic imaging, yet the scarcity of realistic images with ground truth poses poses a significant challenge. Therefore, domain adaptation offers a promising approach to bridge the pre-operative planning domain with the intra-operative real domain for learning odometry information. However, existing methodologies suffer from inefficiencies in the training time. In this work, an efficient neural style transfer framework for endoscopic visual odometry is proposed, which compresses the time from pre-operative planning to testing phase to less than five minutes. For efficient training, this work focuses on training modules with only a limited number of real images and we exploit pre-operative prior information to dramatically reduce training duration. Moreover, during the testing phase, we propose a novel Test Time Adaptation (TTA) method to mitigate the gap in lighting conditions between training and testing datasets. Experimental evaluations conducted on two public endoscope datasets showcase that our method achieves state-of-the-art accuracy in visual odometry tasks while boasting the fastest training speeds. These results demonstrate significant promise for intra-operative surgery applications.

**Keywords:** Endoscopy · Domain adaptation · Efficient training

## 1 Introduction

Monocular Visual Odometry (VO) techniques, employed to infer the ego-motion from a sequence of images, have predominantly been investigated in various applications. However, within endoscopic imaging, the scarcity of *in-vivo* data with ground truth poses notable challenges for deep learning-based VO methods. Recent works mainly address this problem via **unsupervised** and **adaptation** paradigms. The **unsupervised methods** jointly estimates the pose and depth based on Structure-from-Motion (SfM) frameworks [16][1][3][7][9], modeling the correspondence between video frames. Nevertheless, the presence of artifacts and the limited presence of distinctive features in endoscopic environments present significant hurdles [9]. The **adaptation methods** utilizes the synthetic data based on pre-operative scans and transfers them to realistic images[13][14][15][10]. Subsequently, a supervised pose network can be trained using generated realistic images and tested in real intra-operative scenarios. However, existing methods relying on neural style transfer suffer from inefficiency,

characterized by the prolonged training duration as illustrated in Figure 1 (a). Such extensive training periods are suboptimal for practical real-world applications.

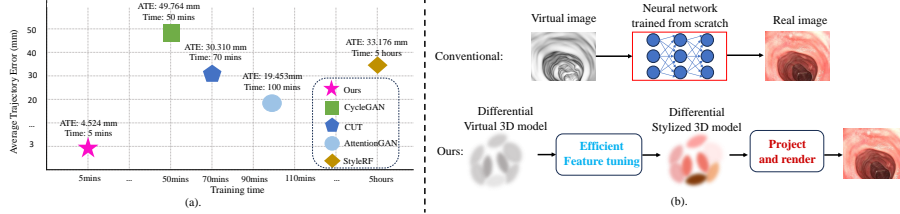


**Fig. 1.** (a) Performance comparison of different methods. “Training time” denotes the duration required for the training of 500 images, and “ATE” refers to the average trajectory error. (b) Comparison between the proposed framework and conventional framework.

In this work, we concentrate on the efficient domain adaptation for endoscopic visual odometry and enhance the training efficiency. The first emphasis lies in utilizing a limited number of real images, thereby substantially reducing training time. Moreover, the proposed method takes advantages of pre-operative structural prior and unlabelled testing images, enabling the efficient training within 5 mins.

Specifically, as shown in Figure 1 (b), in the pre-operative phase, based on Gaussian splatting theory, we reconstruct the differential virtual 3D model, which encompasses parameters representing both texture and structure. Subsequently, we decompose parameters and only refine the texture parameters. This selective optimization of parameters results in a notable reduction in training time while generating high-quality realistic images. In addition, during the testing phase, we propose a novel test time adaptation method, which regards generated random pose as pseudo-label and tunes pose net efficiently.

We summarize our contributions:

- An efficient training strategy for neural style transfer, which decomposes the representation of realistic scene into structural features and texture features, enabling fast optimization.
- A novel test time adaptation method that boosts generalizability of visual odometry network.
- Experiments on two public datasets demonstrate that proposed framework can effectively improve efficiency and accuracy of visual odometry with small amounts of training samples.

## 2 Method

As shown in Figure 2, the proposed framework can be divided into three phases: In the virtual pretraining phase, our framework reconstruct the differential 3D

virtual scene based on 3D Gaussian splatting theory. In the efficient tuning phase, our framework transfer the style from 3D virtual domain into realistic domain, concurrently training a pose net efficiently. Finally, during the testing phase, our framework efficiently tunes the pose net in a unsupervised manner.

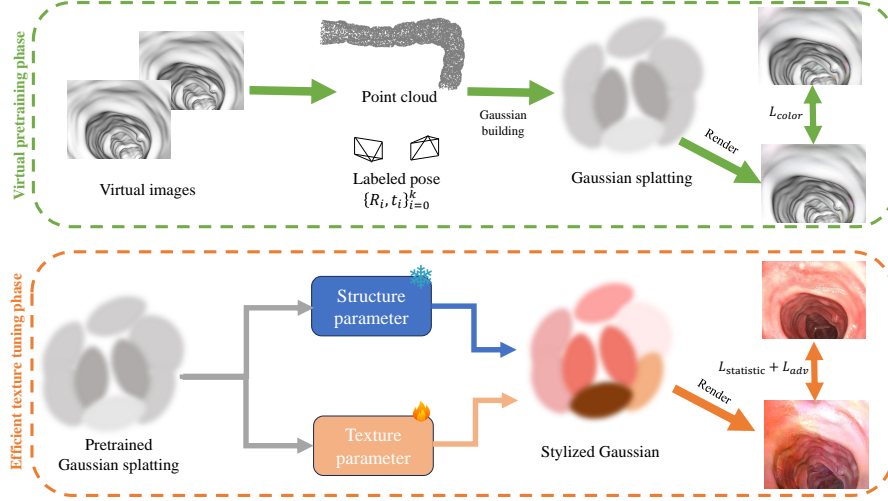


**Fig. 2.** The overall framework of our proposed module. (a). The framework in the virtual pretraining phase. Based on virtual images and poses, the Gaussian module can be built based on Gaussian splatting theory. (b). The parameters of Gaussian module are decomposed by structural parameters and texture parameters. Only texture parameters are optimized during efficient tuning phase.

## 2.1 Virtual pretraining phase

Existing methods commonly reconstruct the pre-operative structures into non-differentiable 3D models such as point clouds or mesh representation, which fails to provide information for intra-operative model. In contrast, in this work, we reconstruct the differential 3D virtual model based on Gaussian splatting theory, which encompasses rich structural information priors.

Gaussian splatting [4] is an explicit 3D scene representation based on a sparse set of SfM points. Given the 3D points, each Gaussian is defined by a 3D covariance matrix  $\Sigma$  and a center point  $x$ :

$$G(x) = e^{-\frac{1}{2}x^T \Sigma^{-1}x} \quad (1)$$

where the covariance matrix  $\Sigma$  can be represented by a rotation matrix  $R$  and a scaling matrix  $S$  for differentiable optimization:

$$\Sigma = R S S^T R^T \quad (2)$$

For projecting 3D Gaussian points to 2D images, the rendering process of N ordered points overlapping a pixel follows a specific formula:

$$C = \sum_{i \in N} c_i \alpha_i \prod_{j=1}^{i-1} (1 - \alpha_j) \quad (3)$$

where  $c_i, \alpha_i$  indicates the color and density of a given point. These parameters are determined by a Gaussian with a covariance matrix  $\Sigma$ , which is then scaled by optimizable per-point opacity and spherical harmonics color coefficients.

To summarize, a 3D scene can be represented by many Gaussian points. Each Gaussian point is characterized by following attributes: position  $\mathbf{x} \in \mathbb{R}^3$ , spherical harmonics coefficients  $\mathbf{c} \in \mathbb{R}^k$  (where k indicates the degree of freedom), opacity  $\alpha \in \mathbb{R}$ , rotation quaternion  $q \in \mathbb{R}^4$ , and a scaling factor  $s \in \mathbb{R}^3$ .

In the virtual pretraining phase, given the labeled virtual images, the Gaussian splatting module is initialized and built based on above formulations. For objective function  $L_{color}$ , we employ MSE loss.

## 2.2 Efficient texture tuning phase

We define the task of 3D style transfer as follows: Given a 3D virtual scene represented by 3D Gaussians, denoted by  $\Theta$ , where each  $\Theta_i = \{x_i, s_i, q_i, \alpha_i, c_i\}$  represents the parameters of the i-th Gaussian as detail in Sec. 2.1. The objective is to achieve an stylized 3D Gaussians, referred to as  $\Theta^y$ , that aligns with the texture of real domain while preserving the original structure.

In the framework, parameters in 3D Gaussian are decomposed into two categories: structure parameters (size, opacity, Gaussian center) and texture parameters (spherical harmonics coefficients). By fixing the structure parameters of the Gaussian, each instance of 3D Gaussian is intend to represent a consistent spatial structure, irrespective of variations in domain texture. Therefore, our framework exclusively finetunes texture parameters during the efficient tuning phase to transfer the representation of domain texture while preserving the stable original structural characteristics. Specifically, two loss functions are designed.

*Statistical loss:* Since the goal of style transfer is to stylize the whole scene such that the generated images are able to demonstrate the similar style with real images, the content loss  $L_{content}$  and the style loss  $L_{style}$  in feature level are designed. Formally, we assume generated realistic image  $I_g$  and virtual image  $I_v$ ,  $L_{content}$  encourage  $I_g$  and  $I_v$  to have similar content features:

$$L_{content} = \|\tau(I_g) - \tau(I_v)\|_2 \quad (4)$$

where  $\tau()$  is the feature representation obtained from the *relu4.1* layer of a pretrained VGG-19 network. In addition, the style loss  $L_{style}$  encourages the mean squared error in terms of feature statistics between generated image  $I_g$  and real image  $I_r$ , to be small:

$$L_{style} = \sum_l \|\mu(\tau_l(I_g)) - \mu(\tau_l(I_r))\|_2 + \sum_l \|\Sigma(\tau_l(I_g)) - \Sigma(\tau_l(I_r))\|_2 \quad (5)$$

where  $\mu$  and  $\Sigma$  represent the mean and standard deviation respectively, and  $\tau_l()$  denotes the feature representation obtained from the  $l$ -th layer of VGG-19.

*Adversarial loss:* Statistical loss focuses on global statistical information, which is unable to match real images in terms of details. To address this issue, we incorporate an adversarial learning loss function:

$$L_D = \mathbb{E}_{y \sim p(I_r)}[\log(D(y))] + \mathbb{E}_{x \sim p(I_g)}[1 - \log(D(g))] \quad (6)$$

$$L_G = \mathbb{E}_{y \sim p(I_g)}[\log(D(y))] \quad (7)$$

Overall, the objective function for the efficient texture tuning phase, in which the gradients are back-propagated to finetune the spherical harmonics coefficients, is then defined as:

$$L_{all} = L_{content} + L_{style} + L_G \quad (8)$$

After getting the stylized 3D Gaussian module, a substantial amount of realistic images with labels can be generated, which can be provided for training the pose net. Since the pose net incorporates the structure information during training phase, in the testing phase, the only inference process is the odometry estimation by pose net.

### 2.3 Test time adaptation based on pose shift

Although generated realistic images are similar to real texture, a notable disjunction in lighting characteristics persists between these synthetic images and real test data. For example, endoscopic images often have specular reflections, which are not easily generated based on clean virtual images. To address this issue, a novel unsupervised test time adaptation is proposed. During the testing phase, the proposed strategy generates a random pose shift  $P$ , then warps the test image to the shifted image using  $P$ . Finally, the training loss is the estimation error between generated pose shift  $P$  and the relative pose between testing image and shifted image estimated by pose net. Specifically, given the test example  $I$ , TTA first generates the pose shift  $P = [R_p | t_p]$ , where  $R_p$  is the rotation matrix and  $t_p$  is the translation vector. Then, for any point  $q = [u, v]$  on testing image  $I$ , the corresponding point  $q'$  on shifted image  $I'$  can be calculated by:

$$q' \sim KPzK^{-1}q \quad (9)$$

where  $K$  is intrinsic parameter of camera, and  $z$  is image depth estimated by supervised neural network.

Overall, the objective function is

$$L_{TTA} = ||R_p - R_{pred}||_2 + \alpha ||t_p - t_{pred}||_2 \quad (10)$$

where  $R_{pred}, t_{pred}$  is the relative pose estimated by pose net.

### 3 Experiment

#### 3.1 Datasets and evaluation

We conduct the experiments on two publicly available datasets, C3VD [2] and EndoSLAM-Unity [7]. C3VD contains 22 small video sequences captured from a real colonoscopy, each accompanied by corresponding virtual models. Virtual images corresponding to real-world counterparts are extracted from virtual 3D models in our experiments. EndoSLAM-Unity provides the Unity environment with different virtual and real textures. We sample 5868 images and split them into 10 videos for training and validation. Our framework is evaluated against various domain adaptation techniques, including test time adaptation methods (DUA [6], CoTTA [12]), and neural style transfer methods (CycleGAN [17], CUT [8], AttentionGAN [11], and StyleRF [5]).

#### 3.2 Results

Both the qualitative analysis of style transfer and quantitative evaluation of pose estimation are validated between proposed method and baselines. The accuracy of pose estimation is firstly presented in Table 1 and Figure 3. The “Training time” column indicates training time when using 500 virtual images and 10 real images as unpaired training samples and “Testing time” is the inference time of each frame. The *virtual only* setting exhibits suboptimal performance owing to the substantial gap between virtual and real domains. In addition, the utilization of a limited number of real images in our experiments results in poor performance of conventional neural style methods, primarily due to the overfitting to the texture features while ignoring keeping the structural features. Conversely, unsupervised test-time adaptation demonstrates enhanced accuracy, underscoring their effectiveness in facilitating domain adaptation. Moreover, empirical evidence suggests that our method significantly outperforms all baseline approaches in pose estimation accuracy, while requiring minimal training time.

Besides, we also visualize the generated realistic images from virtual inputs by different neural style transfer methods. Since the aim is to generate realistic images for training pose net, it is crucial to generate images that are texturally realistic while preserving the original virtual structure. As shown in Figure 4, due to the paucity of real samples, 2D style transfer methods overfit to the texture feature, while ignoring keeping the structure. In addition, 3D style transfer, StyleRF, lacks local detail information as it primarily relies on global statistical features. Conversely, our framework yields realistic textures while preserving the structure.

### 4 Ablation study

In this section, we conduct ablation studies on the C3VD dataset to investigate the key components, *design of objective function* and *test time adaptation strategy*, in our framework and demonstrate their efficacy. Table 2 shows the results of all ablation study.

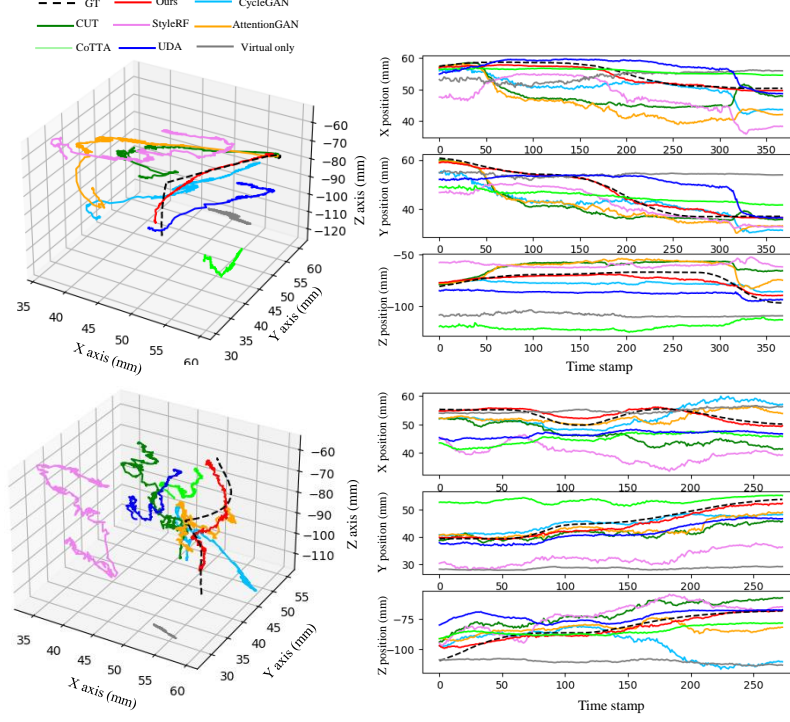


**Fig. 3.** The estimated camera trajectories for two of the testing video sequences by each method in both 3D and x, y, z axis.

**Table 1.** Quantitative results of baselines and proposed method.

Method	Training Time	Testing Time	Dataset					
			C3VD			Unity		
			ATE(mm)	T_rel(mm)	R_rel(deg)	ATE(mm)	T_rpe(mm)	R_rpe(deg)
Virtual only	—	5.011 ms	36.037±19.721	4.787±2.430	4.208±2.315	28.497±13.671	4.508±0.031	4.912±2.746
DUA	—	41.636 ms	19.820±10.843	2.761±1.510	1.979±1.042	16.382±8.390	2.259±1.313	1.845±0.903
CoTTA	—	116.351 ms	17.512±9.581	2.164±1.452	2.001±0.994	12.956±5.730	1.937±0.898	2.583±1.487
CycleGAN	50 mins	5.011 ms	49.764±27.831	6.216±3.857	4.841±2.506	40.594±23.753	5.783±3.014	3.587±2.073
CUT	100 mins	5.011 ms	30.310±13.926	4.729±2.571	2.519±1.374	23.174±11.602	3.710±2.163	2.349±1.174
AttentionGAN	70 mins	5.011 ms	19.453±11.384	2.580±1.053	1.848±1.036	15.881±8.746	2.074±0.941	1.360±0.607
StyleRF	5 hours	5.011 ms	33.176±17.814	3.689±1.012	2.983±1.827	28.945±16.639	2.883±0.980	2.531±1.252
Ours	5 mins	84.455 ms	<b>4.524±2.475</b>	<b>0.601±0.349</b>	<b>0.722±0.491</b>	<b>3.632±0.901</b>	<b>0.491±0.287</b>	<b>0.584±0.286</b>

**Table 2.** Ablation results of proposed modules on the C3VD dataset.

Method	Metric		
	ATE(mm)	T_rel(mm)	R_rel(deg)
w/o statistical loss	6.140±3.144	0.861±0.417	0.984±0.499
w/o adversarial loss	5.082±3.016	0.795±0.523	0.783±0.491
w/o TTA	5.358±2.593	0.813±0.402	0.905±0.478
Ours	4.524±2.475	0.601±0.349	0.722±0.491

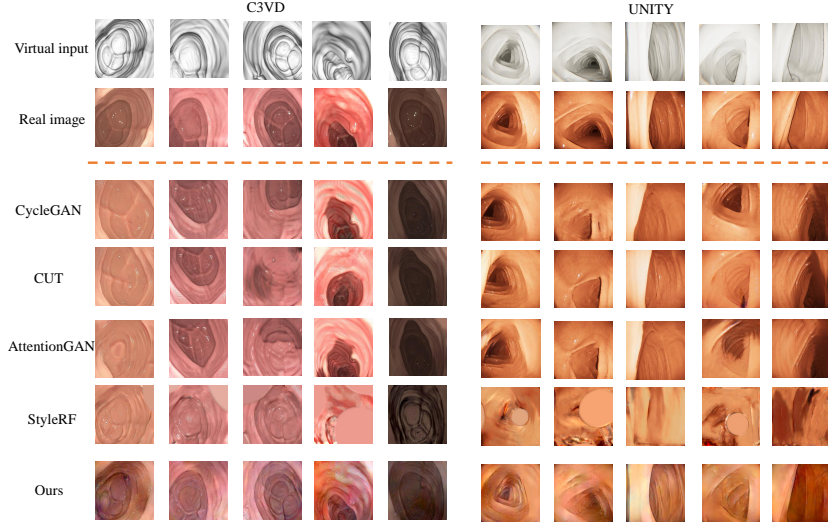


**Fig. 4.** C3VD and EnodoSLAM-Unity example: The generated realistic images from virtual input by the proposed method and baselines for comparison.

The results demonstrate that TTA during testing phase can mitigate the gap between generated training images and testing images, thereby improving the accuracy of pose estimation. In addition, the incorporation of two loss functions has considerable significance. The statistical loss function primarily attends to the overarching textural characteristics of images at a global scale, whereas the adversarial loss function is tailored to address local textural attributes, including intricacies such as folds within cavities and vascular features.

## 5 Conclusion

In this paper, we introduce an efficient and accurate method for intra-operative visual odometry based on 3D neural style transfer. By taking advantage of pre-operative prior and decomposing representation to structural features and texture features, we can efficiently tune virtual textures to realistic textures while keeping the original structure. Our experiments show that proposed module achieves the SOTA accuracy on visual odometry task in just 5 minutes of training, which is over  $10 \times$  faster. We hope that the proposed module holds promise for enhancing navigational capabilities in robotic surgery, which could be advantageous to clinically oriented tasks.

## References

1. Bian, J.W., Zhan, H., Wang, N., Li, Z., Zhang, L., Shen, C., Cheng, M.M., Reid, I.: Unsupervised scale-consistent depth learning from video. *International Journal*

- of Computer Vision **129**(9), 2548–2564 (2021)
2. Bobrow, T.L., Golhar, M., Vijayan, R., Akshintala, V.S., Garcia, J.R., Durr, N.J.: Colonoscopy 3d video dataset with paired depth from 2d-3d registration. *Medical image analysis* **90**, 102956 (2023)
  3. Godard, C., Mac Aodha, O., Firman, M., Brostow, G.J.: Digging into self-supervised monocular depth estimation. In: *Proceedings of the IEEE/CVF international conference on computer vision*. pp. 3828–3838 (2019)
  4. Kerbl, B., Kopanas, G., Leimkühler, T., Drettakis, G.: 3d gaussian splatting for real-time radiance field rendering. *ACM Transactions on Graphics* **42**(4) (2023)
  5. Liu, K., Zhan, F., Chen, Y., Zhang, J., Yu, Y., El Saddik, A., Lu, S., Xing, E.P.: Stylerf: Zero-shot 3d style transfer of neural radiance fields. In: *Proceedings of the IEEE/CVF Conference on Computer Vision and Pattern Recognition*. pp. 8338–8348 (2023)
  6. Mirza, M.J., Micorek, J., Possegger, H., Bischof, H.: The norm must go on: Dynamic unsupervised domain adaptation by normalization. In: *Proceedings of the IEEE/CVF Conference on Computer Vision and Pattern Recognition*. pp. 14765–14775 (2022)
  7. Ozyoruk, K.B., Gokceler, G.I., Bobrow, T.L., Coskun, G., Incetan, K., Almalioglu, Y., Mahmood, F., Curto, E., Perdigoto, L., Oliveira, M., et al.: Endoslam dataset and an unsupervised monocular visual odometry and depth estimation approach for endoscopic videos. *Medical image analysis* **71**, 102058 (2021)
  8. Park, T., Efros, A.A., Zhang, R., Zhu, J.Y.: Contrastive learning for unpaired image-to-image translation. In: *Computer Vision–ECCV 2020: 16th European Conference, Glasgow, UK, August 23–28, 2020, Proceedings, Part IX* 16. pp. 319–345. Springer (2020)
  9. Shao, S., Pei, Z., Chen, W., Zhu, W., Wu, X., Sun, D., Zhang, B.: Self-supervised monocular depth and ego-motion estimation in endoscopy: Appearance flow to the rescue. *Medical image analysis* **77**, 102338 (2022)
  10. Shen, M., Gu, Y., Liu, N., Yang, G.Z.: Context-aware depth and pose estimation for bronchoscopic navigation. *IEEE Robotics and Automation Letters* **4**(2), 732–739 (2019)
  11. Tang, H., Liu, H., Xu, D., Torr, P.H., Sebe, N.: Attentiongan: Unpaired image-to-image translation using attention-guided generative adversarial networks. *IEEE transactions on neural networks and learning systems* (2021)
  12. Wang, Q., Fink, O., Van Gool, L., Dai, D.: Continual test-time domain adaptation. In: *Proceedings of the IEEE/CVF Conference on Computer Vision and Pattern Recognition*. pp. 7201–7211 (2022)
  13. Zhang, J., Liu, L., Xiang, P., Fang, Q., Nie, X., Ma, H., Hu, J., Xiong, R., Wang, Y., Lu, H.: Ai co-pilot bronchoscope robot. *Nature communications* **15**(1), 241 (2024)
  14. Zhang, L., Ratsamee, P., Luo, Z., Uranishi, Y., Higashida, M., Takemura, H.: Panoptic-level image-to-image translation for object recognition and visual odometry enhancement. *IEEE Transactions on Circuits and Systems for Video Technology* (2023)
  15. Zhao, C., Shen, M., Sun, L., Yang, G.Z.: Generative localization with uncertainty estimation through video-ct data for bronchoscopic biopsy. *IEEE Robotics and Automation Letters* **5**(1), 258–265 (2019)
  16. Zhou, T., Brown, M., Snaveley, N., Lowe, D.G.: Unsupervised learning of depth and ego-motion from video. In: *Proceedings of the IEEE conference on computer vision and pattern recognition*. pp. 1851–1858 (2017)

17. Zhu, J.Y., Park, T., Isola, P., Efros, A.A.: Unpaired image-to-image translation using cycle-consistent adversarial networks. In: Proceedings of the IEEE international conference on computer vision. pp. 2223–2232 (2017)